Interaction-Driven Instabilities in the Random-Field *XXZ* Chain

Jeanne Colbois, Fabien Alet, and Nicolas Laflorencie
Laboratoire de Physique Théorique, Université de Toulouse, CNRS, UPS, France

(Received 23 April 2024; accepted 26 July 2024; published 12 September 2024)

Despite enormous efforts devoted to the study of the many-body localization (MBL) phenomenon, the nature of the high-energy behavior of the Heisenberg spin chain in a strong random magnetic field is lacking consensus. Here, we take a step back by exploring the weak interaction limit starting from the Anderson localized (AL) insulator. Through shift-invert diagonalization, we find that, below a certain disorder threshold h^*, weak interactions necessarily lead to an ergodic instability, whereas at strong disorder the AL insulator directly turns into MBL, in agreement with a simple interpretation of the avalanche theory for restoration of ergodicity. We further map the phase diagram for the generic *XXZ* model in the disorder h–interaction Δ plane. Taking advantage of the total magnetization conservation, our results unveil the remarkable behavior of the spin-spin correlation functions: in the regime indicated as MBL by standard observables, their exponential decay undergoes an inversion of orientation $\xi_z > \xi_x$. We find that the longitudinal length ξ_z is a key quantity for capturing ergodic instabilities, as it increases with system size near the thermal phase, in sharp contrast to its transverse counterpart.

DOI: 10.1103/PhysRevLett.133.116502

Introduction—Understanding the subtle interplay between disorder and interactions in quantum systems is a major challenge in condensed matter physics. In particular, the many-body localization (MBL) problem remains a disputed issue, despite almost two decades of study [1–13]. Key debates revolve around the (existence of an) ergodicity-breaking transition at high energies, its possible universality class, and associated finite-size behavior [14–24], as well as the microscopic mechanisms driving the restoration of ergodicity [25–31]. In this context, it is instructive to recall the original concern of the field [3,4,32]: what is the fate of the Anderson localized (AL) insulator against weak interactions? Although this question is well posed, most numerical work has focused instead on the strongly interacting random-field Heisenberg chain (RFHC) [6,14,23,33–41], with few exceptions [42–50]. Over the past decade, the RFHC has gone from the standard model of MBL to an increasingly controversial topic, primarily due to numerical finite-size effects [37,39–41,52,53], and to the observation of very slow dynamics [35,38,54–57] in a regime previously thought to be deeply localized. This led to very different conclusions, such as the absence of a genuine MBL phase [58–60], regardless of mathematical arguments [9,61] in favor of its existence in a related model, and clear signatures of nonthermal behavior in various related experiments [62–69].

Main results—In this Letter, we consider the easy-plane *XXZ* spin chain

$$\mathcal{H}_\Delta = \sum_i \left(S_i^x S_{i+1}^x + S_i^y S_{i+1}^y + \Delta S_i^z S_{i+1}^z + h_i S_i^z\right), \quad (1)$$

with $\Delta \in [0,1]$ ($\Delta = 1$ being the RFHC) and random fields uniformly drawn in $[-h,h]$. $\mathcal{H}_\Delta$ conserves $S^z_{\text{tot}} = \sum_i S_i^z$, which we will highly exploit. Figure 1 presents the high-energy phase diagram of this model, building on midspectrum shift-invert diagonalization [14,70] of periodic chains of sizes $L \in [10, \ldots, 21]$. Before giving a detailed description, we sketch our main findings. (i) Along the noninteracting line $\Delta = 0$, we argue, and numerically verify,

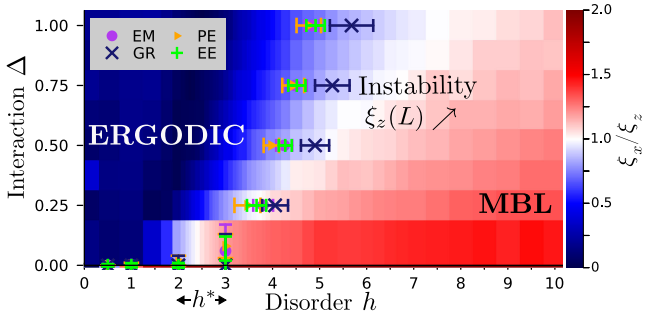

FIG. 1. Disorder-interaction phase diagram of the *XXZ* chain Hamiltonian (1) at high energy (middle of the many-body spectrum, $\epsilon = 0.5$ [14]) in the largest sector $S^z_{\text{tot}} = 0$ (1/2 for odd L). Symbols indicate the ergodic to MBL transition obtained from standard observables (see main text) by extrapolation of the crossings (Figs. 2 and 3, and Supplemental Material [71]). The transition line starts from the Anderson insulator ($\Delta = 0$) at a finite disorder strength h^*. At stronger disorder, the heat map shows the ratio of the transverse to longitudinal midchain correlation lengths, fitted on even sizes $L = 10, \ldots, 16$, starting with $\xi_x/\xi_z \approx 2$ at $\Delta = 0$. The region where $\xi_x/\xi_z \lesssim 1$ roughly matches the instability regime in which $\xi_z(L)$ increases with L (Fig. 3 and main text).

that there is a disorder threshold h^* for the AL insulator below which any finite interaction restores ergodicity, while at strong disorder, AL turns into MBL. (ii) For finite Δ, we provide an extrapolation ($L \to \infty$) of the MBL transition line using standard estimates (Fig. 1). (iii) Spin-spin correlation functions (longitudinal zz and transverse xx, with respect to the random field) and their associated correlation lengths $\xi_{x,z}$ present remarkably contrasted behaviors on the MBL side: the dominant orientation $\xi_x > \xi_z$ (inherited from AL) changes to $\xi_x < \xi_z$ across the phase diagram (see color map in Fig. 1). At intermediate disorder, this is accompanied by a growth of ξ_z with L, while ξ_x barely changes. We interpret these observations as a qualitative sign of increasing ergodic instabilities, based on the behavior of these correlators in the ergodic phase. (iv) For larger h, both AL and MBL show very short and size-independent $\xi_{z,x} \ll 1$, suggesting that an ergodic instability is very unlikely.

Ergodic instability at weak interactions—The most discussed theoretical framework describing the restoration of ergodicity from the MBL phase is provided by the avalanche theory (AT) [27,28]. In a nutshell, the AT starts from strong disorder and considers a possible runaway delocalizing instability triggered by rare ergodic seeds. This is predicted to occur when the length scale ζ, controlling the exponential decay of the effective coupling between the ergodic bubble and the surrounding localized spins, exceeds a certain $\mathcal{O}(1)$ critical threshold ζ_{avl} [78]. A good starting point for estimating ζ is the noninteracting AL limit, since this length scale can be identified [79] to the disorder-dependent many-body AL length [25,80] $\xi_{\mathrm{AL}} = 1/\ln[1 + (h/h_0)^2]$ [81] controlling the exponentially localized Anderson orbitals. A naive application of AT in the vanishing interaction limit, where $\zeta \sim \xi_{\mathrm{AL}}$, predicts the existence of a finite disorder strength below which an instability condition is met. Since the localization length typically increases with the interaction strength [82–84], an interaction-driven ergodic instability seems inevitable below a certain threshold disorder strength h^*. Conversely, at higher disorder, the noninteracting localization length is much smaller and the MBL phase is expected to be stable for weak interactions if they do not enhance the localization length beyond the avalanche criterion [28,79]. Below, we compare these simple ideas with shift-invert results.

Phase diagram from standard observables—We first verify the existence of an ergodic instability at weak disorder for vanishing interaction Δ. Figure 2 displays results for vertical scans at $h = 1, 2$ (where $\xi_{\mathrm{AL}} \approx 1.9, 0.7$). Figures 2(a) and 2(b) display two standard markers for the transition: midchain entanglement entropy and a measure of the spectral statistics based on the Kullback-Leibler (KL) divergence between the gap ratio distribution and the Poisson statistics $\mathrm{KL}_{[P(r)|\mathrm{Poisson}]}$ (Supplemental Material [71]). Figures 2(c) and 2(d) demonstrate a clear drift of the crossing positions for even and odd sizes with increasing L, thus showing that $\Delta_c(L) \to 0$ for $h = 1$ and $h = 2$.

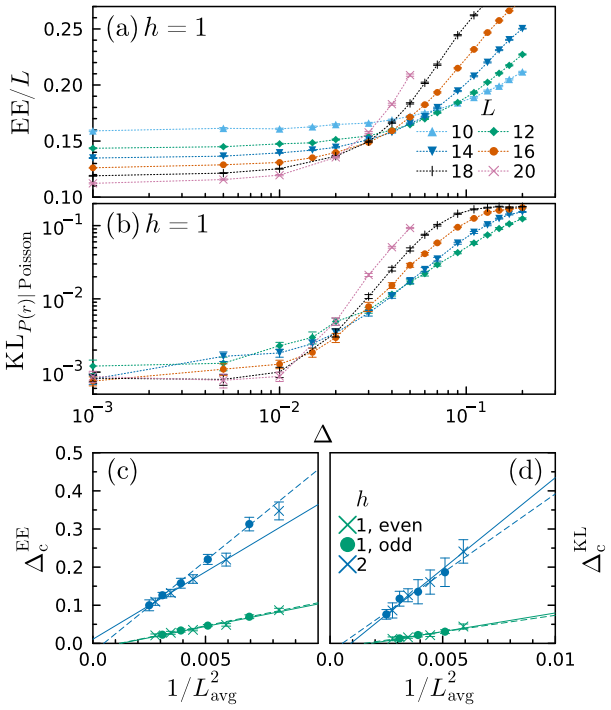

FIG. 2. Critical interaction strength Δ_c above which ergodicity occurs at constant fields ($h = 1, 2$), obtained from midchain entanglement entropy (EE) and gap ratio (GR) statistics. At finite sizes, upon decreasing Δ, (a) EE changes from a volume law at large interaction to an area law at small interaction, and (b) the Kullback-Leibler divergence between the gap ratio distribution and the Poisson statistics goes from ≈0.1895 to ≈0 [71]. (c),(d) Drifts of Δ_c for EE and GR crossings of even (crosses, solid fits) and odd (circle, dashed fits) sizes. L_{avg} indicates the mean of two sizes. The best fits yield a quadratic dependence with $1/L_{\mathrm{avg}}$.

For stronger disorder, the system is in a finite-size crossover regime, yielding very large errors and a strong drift for $\Delta_c(L)$ at $h = 3$, making the extrapolation difficult [71] (see Fig. 1). Although this makes it challenging to extract a precise numerical value for the noninteracting threshold h^*, our data clearly point to a finite and not too small value $2 \leq h^* \leq 3$, corresponding to a short AL length $0.7 \geq \xi_{\mathrm{AL}}^* \geq 0.5$.

In Fig. 1, we report this ergodic instability using two further measures: the eigenstate ergodicity in the Hilbert space quantified by the participation entropy (PE) [14,33,36,85], and the extreme local magnetizations (EM) [23,51,80]. These results bring insight to the observations in Ref. [86] and into the results of Ref. [46], where the reported onset of quantum chaos is naturally explained by the study being performed at low disorder ($h \approx 0.57, \xi \approx 5$). A similar scenario occurs in the disordered interacting Majorana chain, where an immediate ergodic instability arises when the noninteracting localization length exceeds a threshold [48].

Moving away from AL, we investigate the extent of the ergodic regime at finite interaction, building on the same

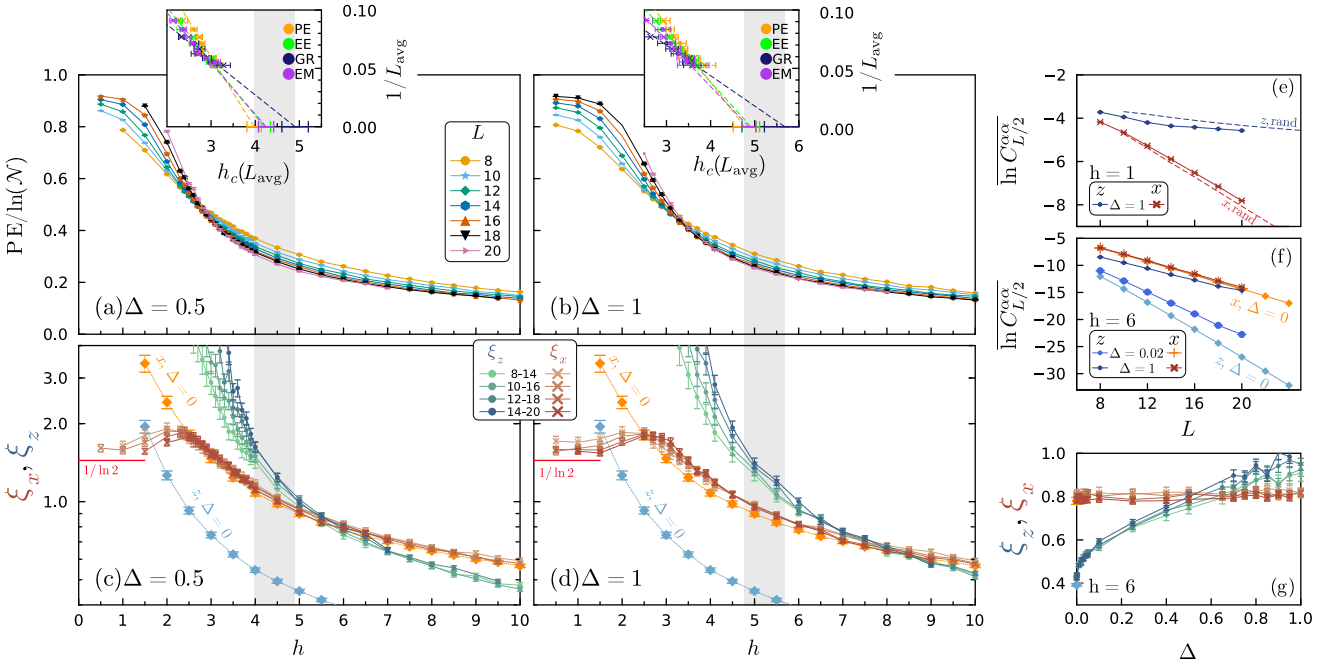

FIG. 3. Overview of the ergodic, MBL, and instabilities regimes. The gray area indicates the critical disorder extrapolated from standard observables (insets). (a),(b) At $\Delta = 0.5$ and $\Delta = 1$, the PE scaling with the logarithm of the Hilbert space dimension $D_1 \ln \mathcal{N} + b_1$ shows a crossing point, corresponding to a change of sign for the subleading correction b_1. (c)–(g) Midchain correlations, Eq. (2), and corresponding correlation lengths, Eq. (3). (c),(d) Correlation lengths at $\Delta = 0.5$ and $\Delta = 1$ compared to the AL case, extracted from fits on even sizes. (e),(f) Associated characteristic correlations decay: (e) ergodic regime at $h = 1$, $\Delta = 1$, compared to an $S_z = 0$ random vector (dashed lines); (f) MBL regime at $h = 6$, $\Delta = 0.02$ and regime showing instabilities at $h = 6$, $\Delta = 1$, compared to the AL correlations for the same disorder strength. (g) At $h = 6$, the longitudinal correlation length shows a square-root-like dependence on Δ. In all cases, the AL values come from fits on $L = 14, \ldots, 20$.

four observables. Figures 3(a) and 3(b) report the PE behavior for various sizes as a function of the disorder h for fixed $\Delta = 0.5$ and $\Delta = 1$ (RFHC). In agreement with previous observations, small system sizes underestimate the ergodic regime, leading to systematic finite-size drifts for the ergodic-to-MBL crossovers toward larger disorder strengths (Supplemental Material [71]), clearly shown in the top insets of Fig. 3. Using linear fits with $1/L$ as in the RFHC case [37], we find that these drifts consistently converge to finite values h_c, indicating a broad but finite extent of the ergodic regime shown by the various symbols in Fig. 1. Note that the spectral statistics systematically yield the largest critical extrapolated disorder strengths h_c^{GR}. For $\Delta = 1$, our estimate $h_c^{\mathrm{GR}} = 5.6(5)$ is consistent with the numerical landmark $h_{\mathrm{mg}} \approx 5.7$ proposed by Morningstar *et al.* [41], where the smallest gap starts to deviate from Poisson expectations.

New insights from spin correlations—Aiming to provide a real-space view of how ergodicity is reached from the strong disorder regime, we now focus on pairwise spin correlations for midspectrum eigenstates of $\mathcal{H}_\Delta$. Introduced early on as possible indicators of the MBL transition for the RFHC [6], correlations have, however, been the subject of surprisingly little work for U(1) symmetric models [6,87–91], leading nonetheless to the observation of their nontrivial distributions in both ergodic and MBL regimes [88] and suggesting they may signal an intermediate critical phase driven by rare events [87].

We show that spin correlations provide remarkable insights, for several reasons. First, exponentially decaying correlators allow one to connect to the noninteracting Anderson limit, where the localization and spin correlation lengths are all proportional (for $h \gtrsim 2$). Moreover, correlation lengths remain well defined in the MBL regime at strong disorder. Finally, correlations at the largest possible distance in periodic chains can probe early onsets of thermalization processes through system-wide resonances. We focus on the midchain connected correlation functions [92]

$$C^{\alpha\alpha}_{L/2} = \left|\langle S^\alpha_i S^\alpha_{i+L/2}\rangle - \langle S^\alpha_i\rangle\langle S^\alpha_{i+L/2}\rangle\right|. \tag{2}$$

Figures 3(e) and 3(f) illustrate the two limiting cases for the characteristic decay with L of the typical average of the longitudinal ($\alpha = z$) and transverse ($\alpha = x$) components. In the ergodic phase, where the eigenstate thermalization hypothesis (ETH) applies [93–95], eigenstates are well described by featureless random states, yielding an absence of spatial variation for both components. However, we expect strongly contrasted dependences on L: while ETH implies an exponential vanishing with the system size for

$C^{xx}_{L/2} \sim \mathcal{N}^{-1/2}$ (with $\mathcal{N} \approx 2^L$ the size of the Hilbert space), the total magnetization conservation ($S^z_{\rm tot} =$ constant) leads to a much slower algebraic decay of the longitudinal component $C^{zz}_{L/2} \sim (4L)^{-1}$. In Fig. 3(e), exact diagonalization results deep in the ergodic regime indeed show different behaviors, approaching the exact calculation performed with $S^z_{\rm tot} = 0$ random states.

Conversely, although the magnetization conservation still holds, the strong disorder regime shows exponential decays for both x and z components, as shown for $h = 6$ and weak enough interaction in Figs. 3(f) and 3(g). It is therefore natural to define the typical midchain correlations lengths ξ_x and ξ_z as follows:

$$\overline{\ln C^{\alpha\alpha}_{L/2}} =: -\frac{L}{2\xi_\alpha} + \mathcal{O}(1), \tag{3}$$

where $\overline{(\ldots)}$ stands for disorder averaging. We first make a few key observations for the large-h, presumably localized regime.

(i) In the noninteracting AL limit ($\Delta = 0$) the z component of the spins is pinned by strong random fields, yielding short correlation lengths and dominant quantum fluctuations in the transverse channel. As a result, we observe at $h = 6$, $\xi^{\rm AL}_x = 0.80(2) > \xi^{\rm AL}_z = 0.41(1)$. This factor of 2 appears to be robust along almost the entire AL line, at least for $h > 2$ (see Fig. 1), providing a hallmark for this regime.

(ii) Remarkably, even a very weak interaction above the AL line leads to a strong qualitative change for the longitudinal correlations with a sharp increase of ξ_z, while the transverse part remains essentially unaffected, as clearly visible in Figs. 3(f) and 3(g). In particular, we observe in Fig. 3(g) a very rapid, square-root-like increase of ξ_z with Δ, while ξ_x approximately keeps its noninteracting value.

(iii) For larger interactions, the trend intensifies so that ξ_z crosses ξ_x around $\Delta \sim 0.5$ and eventually becomes larger as illustrated by the Heisenberg point at $\Delta = 1$, $h = 6$.

Interaction-driven instabilities—This striking reversal in the orientation of the dominant correlations, already visible at small size in the color plot provided over the entire phase diagram, is even more apparent with larger L in Figs. 3(c) and 3(d) where one observes crossing between ξ_x and ξ_z for two representative horizontal cuts ($\Delta = 0.5, 1$). In addition, both plots show that the transverse correlation length ξ_x has a very weak size dependence and remains finite and small everywhere. The only significant interaction effect appears in the ergodic regime below $h \approx 2.5$, where ξ_x deviates from the divergence of $\xi^{\rm AL}_x$ and decays to its ETH value $1/\ln 2$. Quite differently, Figs. 3(c), 3(d), and 3(g) show that the longitudinal correlation length ξ_z is much more sensitive and displays very pronounced variations both with Δ (in all regimes) and with L (in the ergodic phase). The latter is easily understood from the distinction between the algebraic and exponential decay of the typical $C^{zz}_{L/2}$ vs $C^{xx}_{L/2}$ in the ergodic regime, where effectively $\xi_x/\xi_z \to 0$ as L increases.

In the opposite case of strong disorder and weak interaction, the situation is qualitatively very close to AL, with $\xi_x > \xi_z$. This suggests that MBL and AL are connected in this part of the phase diagram [80,96], where, furthermore, no finite-size effects are observed for either ξ_z or ξ_x. However, as the disorder is gradually reduced, though still well before the presumed ergodic transition, an instability is observed via a systematic growth with L of our numerical estimates of ξ_z. This is clearly visible in Fig. 3 where one sees such instabilities, for example, as soon as $h < 7$ for $\Delta = 0.5$ [Fig. 3(c)] or above $\Delta \approx 0.1$ for $h = 6$ [Fig. 3(g)], both cases corresponding to a regime where all other standard finite-size observables show well-converged MBL-like behavior. This striking finding is a stronger signal than the observed $\xi_x = \xi_z$ crossing, even though it occurs in roughly the same regime. Indeed, such a crossing simply reflects the fact that ξ_z increases faster than ξ_x, but the additional growth of ξ_z with L is a remarkable indication of an anomalous response of the diagonal correlations in a regime of disorder where one would have rather expected MBL physics. Based on the very different scaling with L of $C^{zz}_{L/2}$ in the two opposite regimes, we may therefore interpret these observations as a qualitative marker of emerging ergodic instabilities in models conserving the total magnetization.

Summary and discussion—In this Letter, we first provided evidence for the direct instability of the Anderson insulator toward ergodic behavior in the small interaction, weak disorder limit $h < h^* \sim 2$–3. This prediction is directly testable experimentally in platforms with controllable interactions, such as with Feshbach resonances in cold atoms [62,97]. In a second part, we took advantage of the magnetization or particle number conservation (often met in experiments) to unveil a finite-size growing instability of $\xi_z(L)$, in a part of the phase diagram where other finite-size indicators point to an MBL regime. Our main results, summarized in Figs. 1 and 3, will be further detailed and expanded in a forthcoming paper [98]. The system-wide response probed by $C^{zz}_{L/2}$ and its two-body nature can be linked to the end-to-end mutual information [99], which was recently used as a landmark to detect system-wide resonances [41]. Two remarks are in order though: by averaging over eigenstates and disorder realizations, $\ln C^{zz}_{L/2}$ reflects the typical behavior, whereas Ref. [41] studied the extreme statistics of the maximal (over all eigenstates) mutual information. Second, the connected correlator C^{zz} is routinely accessible as a density-density correlation in most MBL experimental platforms, see, e.g., Ref. [66], which indeed observe an increase of ξ_z as disorder is decreased in the MBL regime, albeit in a different setup than ours (correlations after a quench in a quasiperiodic potential vs correlators in eigenstates in a random potential).

Could ξ_z growing with L be further considered a smoking gun of avalanches? Our eigenstates analysis does

not allow us to conclude on this, but we remark that ergodic inclusions (potential seeds for avalanches) naturally favor an enhancement of diagonal correlations. Indeed, typical zz correlations barely decay across ergodic regions, yielding an effective growth of ξ_z, which may be a key quantity to further investigate avalanche instabilities in realistic microscopic models (for a recent study of dynamical correlations in this context, see Ref. [100]). Nevertheless, one of the most difficult remaining questions concerns the status of the intermediate region showing finite-size instabilities. Will the growth of $\xi_z(L)$ continue on larger length scales, giving rise to an ergodic regime or a novel intervening glassy state [49], or will it instead saturate, corresponding to an MBL phase? We hope that our Letter will motivate further explorations in particle number-conserving theoretical models or in experimental platforms susceptible to host an MBL transition.

The following sparse linear algebra libraries were used in this Letter: PETSc [101,102], SLEPc [103,104], MUMPS [105,106], and Strumpack [107].

Acknowledgments—We are glad to acknowledge inspiring discussions with G. Biroli, T. Giamarchi, F. Heidrich-Meisner, T. Prosen, M. Tarzia, and R. Vasseur. This work has been partly supported by the EUR Grant NanoX No. ANR-17-EURE-0009 in the framework of the "Programme des Investissements d'Avenir," is part of HQI initiative, and is supported by France 2030 under the French National Research Agency Award No. ANR-22-PNCQ-0002, and also benefited from the support of the Fondation Simone et Cino Del Duca. We acknowledge the use of HPC resources from CALMIP (Grants No. 2022-P0677 and No. 2023-P0677) and GENCI (Projects No. A0130500225 and No. A0150500225).

[1] B. L. Altshuler, Y. Gefen, A. Kamenev, and L. S. Levitov, Quasiparticle lifetime in a finite system: A nonperturbative approach, Phys. Rev. Lett. **78**, 2803 (1997).
[2] P. Jacquod and D. L. Shepelyansky, Emergence of quantum chaos in finite interacting Fermi systems, Phys. Rev. Lett. **79**, 1837 (1997).
[3] I. V. Gornyi, A. D. Mirlin, and D. G. Polyakov, Interacting electrons in disordered wires: Anderson localization and low-T transport, Phys. Rev. Lett. **95**, 206603 (2005).
[4] D. M. Basko, I. L. Aleiner, and B. L. Altshuler, Metal-insulator transition in a weakly interacting many-electron system with localized single-particle states, Ann. Phys. (Amsterdam) **321**, 1126 (2006).
[5] M. Znidaric, T. Prosen, and P. Prelovsek, Many-body localization in the Heisenberg XXZ magnet in a random field, Phys. Rev. B **77**, 064426 (2008).
[6] A. Pal and D. A. Huse, Many-body localization phase transition, Phys. Rev. B **82**, 174411 (2010).
[7] J. H. Bardarson, F. Pollmann, and J. E. Moore, Unbounded growth of entanglement in models of many-body localization, Phys. Rev. Lett. **109**, 017202 (2012).
[8] R. Nandkishore and D. A. Huse, Many-body localization and thermalization in quantum statistical mechanics, Annu. Rev. Condens. Matter Phys. **6**, 15 (2015).
[9] J. Z. Imbrie, On many-body localization for quantum spin chains, J. Stat. Phys. **163**, 998 (2016).
[10] D. A. Abanin and Z. Papić, Recent progress in many-body localization, Ann. Phys. (Berlin) **529**, 1700169 (2017).
[11] F. Alet and N. Laflorencie, Many-body localization: An introduction and selected topics, C.R. Phys. **19**, 498 (2018).
[12] D. A. Abanin, E. Altman, I. Bloch, and M. Serbyn, Many-body localization, thermalization, and entanglement, Rev. Mod. Phys. **91**, 021001 (2019).
[13] P. Sierant, M. Lewenstein, A. Scardicchio, L. Vidmar, and J. Zakrzewski, Many-body localization in the age of classical computing, arXiv:2403.07111.
[14] D. J. Luitz, N. Laflorencie, and F. Alet, Many-body localization edge in the random-field Heisenberg chain, Phys. Rev. B **91**, 081103(R) (2015).
[15] A. Chandran, C. R. Laumann, and V. Oganesyan, Finite size scaling bounds on many-body localized phase transitions, arXiv:1509.04285.
[16] C. Monthus, Many-body-localization transition in the strong disorder limit: Entanglement entropy from the statistics of rare extensive resonances, Entropy **18**, 122 (2016).
[17] V. Khemani, S. P. Lim, D. N. Sheng, and D. A. Huse, Critical properties of the many-body localization transition, Phys. Rev. X **7**, 021013 (2017).
[18] P. T. Dumitrescu, A. Goremykina, S. A. Parameswaran, M. Serbyn, and R. Vasseur, Kosterlitz-Thouless scaling at many-body localization phase transitions, Phys. Rev. B **99**, 094205 (2019).
[19] A. Goremykina, R. Vasseur, and M. Serbyn, Analytically solvable renormalization group for the many-body localization transition, Phys. Rev. Lett. **122**, 040601 (2019).
[20] A. Morningstar and D. A. Huse, Renormalization-group study of the many-body localization transition in one dimension, Phys. Rev. B **99**, 224205 (2019).
[21] A. Morningstar, D. A. Huse, and J. Z. Imbrie, Many-body localization near the critical point, Phys. Rev. B **102**, 125134 (2020).
[22] M. Schiró and M. Tarzia, Toy model for anomalous transport and Griffiths effects near the many-body localization transition, Phys. Rev. B **101**, 014203 (2020).
[23] N. Laflorencie, G. Lemarié, and N. Macé, Chain breaking and Kosterlitz-Thouless scaling at the many-body localization transition in the random-field Heisenberg spin chain, Phys. Rev. Res. **2**, 042033(R) (2020).
[24] I. García-Mata, J. Martin, O. Giraud, B. Georgeot, R. Dubertrand, and G. Lemarié, Critical properties of the Anderson transition on random graphs: Two-parameter scaling theory, Kosterlitz-Thouless type flow, and many-body localization, Phys. Rev. B **106**, 214202 (2022).
[25] A. C. Potter, R. Vasseur, and S. A. Parameswaran, Universal properties of many-body delocalization transitions, Phys. Rev. X **5**, 031033 (2015).
[26] R. Vosk, D. A. Huse, and E. Altman, Theory of the many-body localization transition in one-dimensional systems, Phys. Rev. X **5**, 031032 (2015).

[27] W. De Roeck and F. Huveneers, Stability and instability towards delocalization in many-body localization systems, Phys. Rev. B **95**, 155129 (2017).
[28] T. Thiery, F. Huveneers, M. Müller, and W. De Roeck, Many-body delocalization as a quantum avalanche, Phys. Rev. Lett. **121**, 140601 (2018).
[29] S. Roy, J. T. Chalker, and D. E. Logan, Percolation in Fock space as a proxy for many-body localization, Phys. Rev. B **99**, 104206 (2019).
[30] S. Roy and D. E. Logan, Fock-space correlations and the origins of many-body localization, Phys. Rev. B **101**, 134202 (2020).
[31] H. Ha, A. Morningstar, and D. A. Huse, Many-body resonances in the avalanche instability of many-body localization, Phys. Rev. Lett. **130**, 250405 (2023).
[32] L. Fleishman and P. W. Anderson, Interactions and the Anderson transition, Phys. Rev. B **21**, 2366 (1980).
[33] A. D. Luca and A. Scardicchio, Ergodicity breaking in a model showing many-body localization, Europhys. Lett. **101**, 37003 (2013).
[34] J. Gray, S. Bose, and A. Bayat, Many-body localization transition: Schmidt gap, entanglement length, and scaling, Phys. Rev. B **97**, 201105(R) (2018).
[35] E. V. H. Doggen, F. Schindler, K. S. Tikhonov, A. D. Mirlin, T. Neupert, D. G. Polyakov, and I. V. Gornyi, Many-body localization and delocalization in large quantum chains, Phys. Rev. B **98**, 174202 (2018).
[36] N. Macé, F. Alet, and N. Laflorencie, Multifractal scalings across the many-body localization transition, Phys. Rev. Lett. **123**, 180601 (2019).
[37] P. Sierant, M. Lewenstein, and J. Zakrzewski, Polynomially filtered exact diagonalization approach to many-body localization, Phys. Rev. Lett. **125**, 156601 (2020).
[38] T. Chanda, P. Sierant, and J. Zakrzewski, Time dynamics with matrix product states: Many-body localization transition of large systems revisited, Phys. Rev. B **101**, 035148 (2020).
[39] P. Sierant, D. Delande, and J. Zakrzewski, Thouless time analysis of Anderson and many-body localization transitions, Phys. Rev. Lett. **124**, 186601 (2020).
[40] D. A. Abanin, J. H. Bardarson, G. De Tomasi, S. Gopalakrishnan, V. Khemani, S. A. Parameswaran, F. Pollmann, A. C. Potter, M. Serbyn, and R. Vasseur, Distinguishing localization from chaos: Challenges in finite-size systems, Ann. Phys. (Amsterdam) **427**, 168415 (2021).
[41] A. Morningstar, L. Colmenarez, V. Khemani, D. J. Luitz, and D. A. Huse, Avalanches and many-body resonances in many-body localized systems, Phys. Rev. B **105**, 174205 (2022).
[42] D. Pekker, G. Refael, E. Altman, E. Demler, and V. Oganesyan, Hilbert-glass transition: New universality of temperature-tuned many-body dynamical quantum criticality, Phys. Rev. X **4**, 011052 (2014).
[43] J. A. Kjäll, J. H. Bardarson, and F. Pollmann, Many-body localization in a disordered quantum Ising chain, Phys. Rev. Lett. **113**, 107204 (2014).
[44] R. Sahay, F. Machado, B. Ye, C. R. Laumann, and N. Y. Yao, Emergent ergodicity at the transition between many-body localized phases, Phys. Rev. Lett. **126**, 100604 (2021).
[45] S. Moudgalya, D. A. Huse, and V. Khemani, Perturbative instability towards delocalization at phase transitions between MBL phases, arXiv:2008.09113.
[46] T. LeBlond, D. Sels, A. Polkovnikov, and M. Rigol, Universality in the onset of quantum chaos in many-body systems, Phys. Rev. B **104**, L201117 (2021).
[47] T. B. Wahl, F. Venn, and B. Béri, Local integrals of motion detection of localization-protected topological order, Phys. Rev. B **105**, 144205 (2022).
[48] N. Laflorencie, G. Lemarié, and N. Macé, Topological order in random interacting Ising-Majorana chains stabilized by many-body localization, Phys. Rev. Res. **4**, L032016 (2022).
[49] G. Biroli, A. K. Hartmann, and M. Tarzia, Large-deviation analysis of rare resonances for the many-body localization transition, Phys. Rev. B **110**, 014205 (2024).
[50] Note also a study of the RHFC as a function of the filling [51].
[51] M. Hopjan, G. Orso, and F. Heidrich-Meisner, Detecting delocalization-localization transitions from full density distributions, Phys. Rev. B **104**, 235112 (2021).
[52] R. K. Panda, A. Scardicchio, M. Schulz, S. R. Taylor, and M. Žnidarič, Can we study the many-body localisation transition?, Europhys. Lett. **128**, 67003 (2020).
[53] J. Suntajs, J. Bonca, T. Prosen, and L. Vidmar, Ergodicity breaking transition in finite disordered spin chains, Phys. Rev. B **102**, 064207 (2020).
[54] F. Weiner, F. Evers, and S. Bera, Slow dynamics and strong finite-size effects in many-body localization with random and quasiperiodic potentials, Phys. Rev. B **100**, 104204 (2019).
[55] M. Kiefer-Emmanouilidis, R. Unanyan, M. Fleischhauer, and J. Sirker, Evidence for unbounded growth of the number entropy in many-body localized phases, Phys. Rev. Lett. **124**, 243601 (2020).
[56] D. J. Luitz and Y. B. Lev, Absence of slow particle transport in the many-body localized phase, Phys. Rev. B **102**, 100202(R) (2020).
[57] P. Sierant and J. Zakrzewski, Challenges to observation of many-body localization, Phys. Rev. B **105**, 224203 (2022).
[58] J. Suntajs, J. Bonca, T. Prosen, and L. Vidmar, Quantum chaos challenges many-body localization, Phys. Rev. E **102**, 062144 (2020).
[59] D. Sels and A. Polkovnikov, Dynamical obstruction to localization in a disordered spin chain, Phys. Rev. E **104**, 054105 (2021).
[60] A. Weisse, R. Gerstner, and J. Sirker, Operator spreading and the absence of many-body localization, arXiv:2401.08031.
[61] J. Z. Imbrie, Diagonalization and many-body localization for a disordered quantum spin chain, Phys. Rev. Lett. **117**, 027201 (2016).
[62] M. Schreiber, S. S. Hodgman, P. Bordia, H. P. Lüschen, M. H. Fischer, R. Vosk, E. Altman, U. Schneider, and I. Bloch, Observation of many-body localization of interacting fermions in a quasirandom optical lattice, Science **349**, 842 (2015).

[63] J. Smith, A. Lee, P. Richerme, B. Neyenhuis, P. W. Hess, P. Hauke, M. Heyl, D. A. Huse, and C. Monroe, Many-body localization in a quantum simulator with programmable random disorder, Nat. Phys. **12**, 907 (2016).
[64] H. P. Lüschen, P. Bordia, S. Scherg, F. Alet, E. Altman, U. Schneider, and I. Bloch, Observation of slow dynamics near the many-body localization transition in one-dimensional quasiperiodic systems, Phys. Rev. Lett. **119**, 260401 (2017).
[65] P. Roushan *et al.*, Spectroscopic signatures of localization with interacting photons in superconducting qubits, Science **358**, 1175 (2017).
[66] A. Lukin, M. Rispoli, R. Schittko, M. E. Tai, A. M. Kaufman, S. Choi, V. Khemani, J. Léonard, and M. Greiner, Probing entanglement in a many-body-localized system, Science **364**, 256 (2019).
[67] M. Rispoli, A. Lukin, R. Schittko, S. Kim, M. E. Tai, J. Léonard, and M. Greiner, Quantum critical behaviour at the many-body localization transition, Nature (London) **573**, 385 (2019).
[68] Q. Guo, C. Cheng, Z.-H. Sun, Z. Song, H. Li, Z. Wang, W. Ren, H. Dong, D. Zheng, Y.-R. Zhang *et al.*, Observation of energy-resolved many-body localization, Nat. Phys. **17**, 234 (2020).
[69] J. Léonard, S. Kim, M. Rispoli, A. Lukin, R. Schittko, J. Kwan, E. Demler, D. Sels, and M. Greiner, Probing the onset of quantum avalanches in a many-body localized system, Nat. Phys. **19**, 481 (2023).
[70] F. Pietracaprina, N. Macé, D. J. Luitz, and F. Alet, Shift-invert diagonalization of large many-body localizing spin chains, SciPost Phys. **5**, 045 (2018).
[71] See Supplemental Material at http://link.aps.org/supplemental/10.1103/PhysRevLett.133.116502 which includes Refs. [72–77], for details on the gap ratio and extreme magnetization, on the location of the crossings, and on the number of samples and eigenstates.
[72] C. A. Müller and D. Delande, Disorder and interference: Localization phenomena, arXiv:1005.0915.
[73] N. Rosenzweig and C. E. Porter, "Repulsion of energy levels" in complex atomic spectra, Phys. Rev. **120**, 1698 (1960).
[74] V. Oganesyan and D. A. Huse, Localization of interacting fermions at high temperature, Phys. Rev. B **75**, 155111 (2007).
[75] O. Giraud, N. Mace, E. Vernier, and F. Alet, Probing symmetries of quantum many-body systems through gap ratio statistics, Phys. Rev. X **12**, 011006 (2022).
[76] Y. Y. Atas, E. Bogomolny, O. Giraud, and G. Roux, Distribution of the ratio of consecutive level spacings in random matrix ensembles, Phys. Rev. Lett. **110**, 084101 (2013).
[77] S. Kullback and R. A. Leibler, On information and sufficiency, Ann. Math. Stat. **22**, 79 (1951).
[78] The precise value of ζ_{avl} is set by the many-body level spacing, and depends on the modelization of the coupling between the ergodic seed and the localized spins.
[79] P. J. D. Crowley and A. Chandran, Avalanche induced coexisting localized and thermal regions in disordered chains, Phys. Rev. Res. **2**, 033262 (2020).
[80] J. Colbois and N. Laflorencie, Breaking the chains: Extreme value statistics and localization in random spin chains, Phys. Rev. B **108**, 144206 (2023).
[81] This expression comes from a single fit capturing both strong and weak disorder limits of the many-body AL length, with $h_0 \sim 1.2$ (Supplemental Material [71]).
[82] D. L. Shepelyansky, Coherent propagation of two interacting particles in a random potential, Phys. Rev. Lett. **73**, 2607 (1994).
[83] K. Frahm, A. Müller-Groeling, and J.-L. Pichard, Effective sigma model formulation for two interacting electrons in a disordered metal, Phys. Rev. Lett. **76**, 1509 (1996).
[84] Dietmar Weinmann, Jean-Louis Pichard, and Yoseph Imry, Thouless numbers for few-particle systems with disorder and interactions, J. Phys. I (France) **7**, 1559 (1997).
[85] F. Pietracaprina and N. Laflorencie, Hilbert-space fragmentation, multifractality, and many-body localization, Ann. Phys. (Amsterdam) **435**, 168502 (2021).
[86] S.-H. Lin, B. Sbierski, F. Dorfner, C. Karrasch, and F. Heidrich-Meisner, Many-body localization of spinless fermions with attractive interactions in one dimension, SciPost Phys. **4**, 002 (2018).
[87] S. P. Lim and D. N. Sheng, Many-body localization and transition by density matrix renormalization group and exact diagonalization studies, Phys. Rev. B **94**, 045111 (2016).
[88] L. Colmenarez, P. A. McClarty, M. Haque, and D. J. Luitz, Statistics of correlation functions in the random Heisenberg chain, SciPost Phys. **7**, 064 (2019).
[89] B. Villalonga and B. K. Clark, Characterizing the many-body localization transition through correlations, arXiv:2007.06586.
[90] A. K. Kulshreshtha, A. Pal, T. B. Wahl, and S. H. Simon, Approximating observables on eigenstates of large many-body localized systems, Phys. Rev. B **99**, 104201 (2019).
[91] V. K. Varma, A. Raj, S. Gopalakrishnan, V. Oganesyan, and D. Pekker, Length scales in the many-body localized phase and their spectral signatures, Phys. Rev. B **100**, 115136 (2019).
[92] We follow [6,87] in using the absolute value of the correlations to access the typical behavior. See Supplemental Material [71].
[93] J. M. Deutsch, Quantum statistical mechanics in a closed system, Phys. Rev. A **43**, 2046 (1991).
[94] M. Srednicki, Chaos and quantum thermalization, Phys. Rev. E **50**, 888 (1994).
[95] M. Rigol, V. Dunjko, and M. Olshanii, Thermalization and its mechanism for generic isolated quantum systems, Nature (London) **452**, 854 (2008).
[96] G. De Tomasi, F. Pollmann, and M. Heyl, Efficiently solving the dynamics of many-body localized systems at strong disorder, Phys. Rev. B **99**, 241114(R) (2019).
[97] C. Chin, R. Grimm, P. Julienne, and E. Tiesinga, Feshbach resonances in ultracold gases, Rev. Mod. Phys. **82**, 1225 (2010).
[98] J. Colbois, F. Alet, and N. Laflorencie (to be published).
[99] G. De Tomasi, S. Bera, J. H. Bardarson, and F. Pollmann, Quantum mutual information as a probe for many-body localization, Phys. Rev. Lett. **118**, 016804 (2017).

[100] T. Szołdra, P. Sierant, M. Lewenstein, and J. Zakrzewski, Catching thermal avalanches in the disordered *XXZ* model, Phys. Rev. B **109**, 134202 (2024).

[101] S. Balay *et al.*, PETSc/TAO users manual, Technical Report No. ANL-21/39—Revision 3.20, Argonne National Laboratory, 2023.

[102] S. Balay, W. D. Gropp, L. C. McInnes, and B. F. Smith, Efficient management of parallelism in object oriented numerical software libraries, in *Modern Software Tools in Scientific Computing*, edited by E. Arge, A. M. Bruaset, and H. P. Langtangen (Birkhäuser Press, Boston, 1997), pp. 163–202.

[103] V. Hernandez, J. E. Roman, and V. Vidal, SLEPc: A scalable and flexible toolkit for the solution of eigenvalue problems, ACM Trans. Math. Softw. **31**, 351 (2005).

[104] J. E. Roman, C. Campos, L. Dalcin, E. Romero, and A. Tomas, SLEPc users manual, Technical Report No. DSIC-II/24/02—Revision 3.20, D. Sistemes Informàtics i Computació, Universitat Politècnica de València, 2023.

[105] P. Amestoy, I. S. Duff, J. Koster, and J.-Y. L'Excellent, A fully asynchronous multifrontal solver using distributed dynamic scheduling, SIAM J. Matrix Anal. Appl. **23**, 15 (2001).

[106] P. Amestoy, A. Buttari, J.-Y. L'Excellent, and T. Mary, Performance and scalability of the block low-rank multifrontal factorization on multicore architectures, ACM Trans. Math. Softw. **45**, 2 (2019).

[107] P. Ghysels, X. S. Li, F.-H. Rouet, S. Williams, and A. Napov, An efficient multicore implementation of a novel hss-structured multifrontal solver using randomized sampling, SIAM J. Sci. Comput. **38**, S358 (2016).